Cellulose (2023) 30:5157–5170
https://doi.org/10.1007/s10570-023-05171-2

ORIGINAL RESEARCH

Highly hydrophobic and moisture barrier nanocellulose based films produced via spray deposition

Humayun Nadeem · Mostafa Dehghani · Simin Miri · Mahdieh Pazirofteh · Gil Garnier · Warren Batchelor

Received: 9 May 2022 / Accepted: 22 March 2023 / Published online: 13 April 2023

Abstract Nanocellulose (NC) films are gaining popularity in recent years owing to their recyclability and biodegradability; however, the commercialization of this material is limited by environmental and moisture barrier constraints. The incorporation of carboxymethyl cellulose (CMC) with NC significantly improved the barrier performance but the resultant films were quite hydrophilic and hence completely disintegrated in water. The aim of this study is to produce hydrophobic NC/CMC films without compromising their barrier characteristics. For this purpose, the optimized content of alkyl ketene dimer (AKD) was spray-deposited on the fully and partially dried NC/CMC films and their hydrophobic, barrier and mechanical properties were assessed. The deposition of AKD has improved the hydrophobicity and flexibility while maintaining the barrier properties of the films. However, their tensile index values decreased by 26–29% as compared with the neat NC/CMC films, but the values remained in acceptable range. Additionally, the partially dried spray deposited AKD-NC/CMC films have shown superior results as they showed higher hydrophobicity ($\theta = 127° \pm 3$), while lower percentage of mass loss after immersion for 48 h in water (15%) as compared with the fully dried spray deposited AKD-NC/CMC films.

Supplementary Information The online version contains supplementary material available at https://doi.org/10.1007/s10570-023-05171-2.

H. Nadeem · M. Dehghani · S. Miri · G. Garnier · W. Batchelor (✉)
Department of Chemical and Biological Engineering, Bioresource Processing Research Institute of Australia (BioPRIA), Monash University, Melbourne, VIC 3800, Australia
e-mail: Warren.Batchelor@monash.edu

M. Pazirofteh
Banaszak Holl Group, Department of Chemical and Biological Engineering, Monash University, Melbourne, VIC 3800, Australia

Graphical abstract

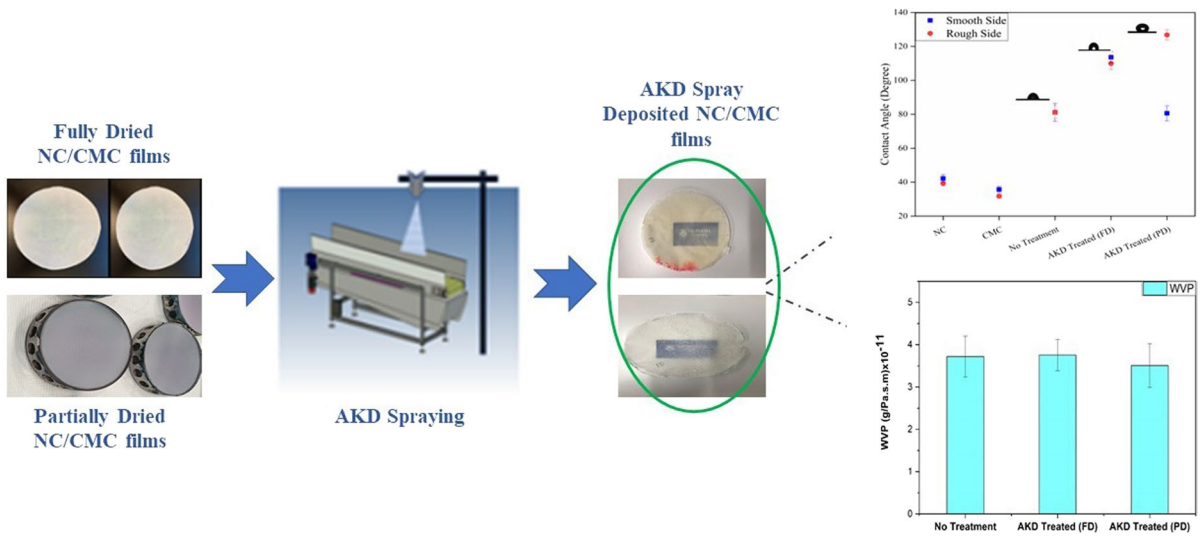

Keywords Alkyl ketene dimer · Carboxy methyl cellulose · Contact angle · Hydrophobicity · Nanocellulose · Spray deposition

Introduction

The development in industrial activities results in surging wastes, that are accumulating in the environment due to the discharge of used products after human consumption. Plastic waste is one of the largest waste streams and its accumulation in the environment is a serious environmental concern (Zhang and Zhao et al. 2021). Plastics are the first choice as packaging materials owing to their exceptional characteristics such as durability, resistance to erosion, low cost and ease of processing (Ho et al. 2018), and their demand continues to increase. According to one estimate, plastic production is expected to increase from 360 million tons in 2018 to 445 million tons in 2025 (Muñoz Meneses et al. 2022). However, around 60% of the plastic is discarded to the environment as plastic waste (Geyer et al. 2017) and at a present trend, the mass of waste plastic is expected to double within the next two decades as this waste cannot be easily recycled or incinerated (Lebreton and Andrady 2019). Majority of the plastic waste is dumped off into landfills, where it undergoes very slow degradation and remains there for extended periods, consequently causing serious environmental changes (Geyer et al. 2017). Additionally, the production of plastics is an energy intensive process, having an overall higher embodied energy (Hammond and Jones 2008; Nadeem et al. 2022). Due to these concerns with current fossil fuel-based plastics, there is a significant interest in transferring to biomass feedstock to produce plant-based packaging.

Among all natural polymers, cellulose is the most abundant having remarkable characteristics such as sustainability, biodegradability, renewability etc. (Shak et al. 2018). Cellulose chains are fibrillated to form cellulose nanomaterials or nanocelluloses with large surface area useful for various application (Foster et al. 2018). One type of cellulose nanomaterials is fibrous nanocellulose (NC) that possess remarkable properties such as low density (Lee et al. 2009; Nechyporchuk et al. 2016; Nogi et al. 2009), none or low toxicity (DeLoid et al. 2019; Liu et al. 2019) and recyclability (Savadekar et al. 2012). The films produced from fibrous NC exhibit translucency, strength and reasonable oxygen barrier characteristics (Shanmugam et al. 2018). Casting and vacuum filtration are the conventional

methods to produce these films (Shanmugam et al. 2017). The casting has two major limitations such as a large timeframe for production and lack of uniformity in the produced films (Shimizu et al. 2014). Contrary, the vacuum filtration is a better process as it rapidly produces high strength films but suffers the handling and intensive labor constrains (Siró and Plackett 2010). Owing to its rapidity and simplicity, spray deposition is regarded as a prospective alternative to conventional methods (Nadeem et al. 2022; Shanmugam et al. 2017). In this process, the NC suspension is sprayed onto a base surface (templates, stainless steel plates etc.) and the magnitude of coating can be altered via two parameters of suspension concentration and the velocity of the conveyor (Shanmugam et al. 2018, 2017).

Due to its distinguishing characteristics, NC is an attractive material for unlimited applications, but there are a number of challenges associated with its use for future applications (Miri et al. 2021, 2022). For instance, the NC films possess limited moisture barrier performance due to the hydrophilic nature of cellulose (Li et al. 2015). Additionally, peeling-off these films from the base surface is occasionally difficult. To overcome these issues, producing composites of NC with compatible materials is considered as a feasible approach (Khan et al. 2014; Miri et al. 2023). Cellulose ether derivatives, particularly carboxymethyl cellulose (CMC), are considered as attractive alternatives to substitute the non-degradable polymer for various applications (Gregorová et al. 2015; Shahbazi et al. 2016). CMC is a seminatural, inexpensive and non-toxic material and is regarded as a compatible additive to produce transparent films (Mandal and Chakrabarty 2018; Zhang et al. 2014). Although, these NC-CMC based films have shown remarkable barrier and mechanical properties, but poor water resistance, making them weak options as replacement for conventional non-degradable polymers (Nadeem et al. 2020; Shahbazi et al. 2016). Multilayered films of different materials are a possible solutions to overcome the limited water resistance and are highly common in packaging industry (Lavoine et al. 2014). Alkyl ketene dimer (AKD) is known for its effect to producing hydrophobic paper under neutral pH conditions (Kumar et al. 2016). AKD can react with free hydroxyl groups, forming β-ketoester linkages, and thus imparting hydrophobicity to cellulose (Takihara et al. 2007; Yoshida and Isogai 2013). It is also observed that the AKD did not change the properties when bonded to cellulose matrix after thermal curing (Yan et al. 2016).

The aim of this study is to produce NC-based hydrophobic and sustainable films via spray deposition for packaging applications. NC/CMC composites were produced to improve the properties and peel ability of the NC films. The composite films, either partial or fully dried, were then surface treated with AKD to produce hydrophobic films. Finally, the mechanical, barrier and morphological properties of these novel AKD treated composite films were compared with those of the NC and NC/CMC composite films. Moreover, the hydrophobicity of the films was determined and compared by degradation test and contact angle analysis.

Materials and methods

Materials

Several terminologies for nanocellulose have been frequently reported in the literature. Most commonly, this material is also named as nano-fibrillated cellulose, cellulose nano-fibrils, and micro fibrillated cellulose etc. (Shanmugam et al. 2017). However, for this research study, the generic term we are using is nanocellulose (NC) for this nanomaterial family. The NC (KY-100S grade) having 25 wt.% solid content were procured from DAICEL Chemical Industries Limited (Japan). NC is speculated to be obtained from cotton source and treated via high pressure homogenization (Hideno et al. 2016; Jang et al. 2015). The commercial grade NC had a mean diameter of approximately 73 nm (Varanasi et al. 2013), while the zeta potential of its suspension was calculated as −22.3 mV (Raj et al. 2017). Moreover, the average aspect ratio of this material was in the range of 142 ± 28 and calculated crystallinity index of about 78% (Shanmugam et al. 2018). The SEM images of NC films at different magnifications is included in the supplementary information (Figure S1). Carboxymethyl cellulose (CMC; FINNFIX 30 g grade), having a percentage purity of 98%, a molecular weight of 80,000, and a degree of substitution (DS) of 0.8 was purchased from CP Kelco (Finland). The commercially available CMC usually have DS in the range of 0.38–1.4 and DS values of 0.6–0.95 are typical

used for food applications (Stephen 1995). The CMC becomes completely soluble at DS above 0.4, while the swelling of the CMC was seen at DS values of below 0.4. Based on these considerations, DS value of 0.8 for CMC was selected in this study. Alkenyl ketene dimer (AKD) having 17% solid content was obtained from Solenis Pty. Ltd. (Australia) and used as the hydrophobization agent. The AKD was further diluted in water to have different concentrations.

Fabrication procedure

Production of NC/CMC films

The CMC powder was slowly mixed with water at 600 RPM in a Eurostar mixer (Germany) and formulating solutions at a 0.9 wt.% concentration of CMC. The concentration of 0.9 wt.% was chosen based on our observation from the previous work, which showed that the films having 5:3 NC/CMC were considerably less dispersed, while 1:1 NC/CMC films were completely disintegrated, when saturated with water (Nadeem et al. 2020). The fibres were then added into the CMC solution to attain the NC/CMC final weight ratio of 5:3, having a total solid content of 1.5 wt.% in the mixture. The suspension was disintegrated in a MK IIIC Messmer disintegrator (Netherlands) for 15,000 revolutions and the resulting suspension had a pH of approximately 6.5. The suspension was sprayed using a Wagner spray system (Shanmugam et al. 2018, 2017) and the sprayed wet films were collected onto circular stainless-steel plates and carried away by a moving conveyor belt. The circular stainless-steel plates had a diameter of 160 mm, while the distance of the nozzle tip from these plates was around 30 cm. The speed of conveyor belt was set at 0.65 cm/sec while the spray nozzle had an orifice of 0.38 mm. The sprayed plates were then finally transferred to an oven (S.E.M Equipment, Australia) for drying at 75 °C for 2 h.

Optimization of AKD

The dried NC/CMC films were placed on stainless steel plates and AKD having different concentrations (1.7, 5.1 and 8.5 wt.%) was sprayed to achieve the (NC/CMC)/AKD final weight ratios of 1:1.13, 1:3.40 and 1:5.66. The sprayed plates were carried away by a moving conveyor belt, while forming an AKD layer at the top of the NC/CMC composite films. To avoid a thick layer of AKD on NC/CMC composite films, the speed of the conveyor belt was double the one used for NC/CMC films i.e., 1.30 cm/sec. The sprayed AKD films were then transferred to an oven for drying at 100 °C for 20 min. The dried films were then subjected to water resistance test for the optimization of AKD. The detail procedure of the test will be discussed in the later section.

Two approaches for AKD deposition

The optimized AKD content was sprayed on NC/CMC films via spray deposition using a spray system. Two approaches were employed for this purpose a) AKD deposition on fully dried (FD) NC/CMC films b) AKD deposition on partially dried (PD) NC/CMC films. For AKD deposition on fully dried NC/CMC films, the optimized content of AKD was sprayed on fully dried NC/CMC films using the same procedure as mentioned in previous section. For the second approach, the NC/CMC suspensions were partially dried at 75 °C for 1 h (≈52%) and the optimized AKD content was sprayed on them via a spray system and carried by a moving belt conveyor (1.30 cm/s). Finally, the wet films were transferred to an oven for drying at 100 °C for 20 min.

Testing procedure

Basis weight and thickness

The basis weight of the films was calculated by dividing their weight to surface area. Prior to basis weight determination, the films were oven-dried at 105 °C for 4 h to remove any traces of moisture. Additionally, a Lorentzen & Wettre AB (Sweden) Thickness Tester was used to calculate the thickness of the films in accordance with Australian/New Zealand standard method 426 (AS/NZS-426 1994).

Water resistance

The water resistance values of the films were calculated in terms of total soluble matter and expressed as the weight percentage of the films solubilized after 1 and 2 days of immersion in distilled water. The dried films were cut into strips (100 mm × 15 mm), weighed and placed in a container containing 250 ml

of water. The assemblies were then transferred to a normal operating temperature of refrigerator (4 °C) for 24 h. After 1 day, the strips from the water container kept in a fridge were transferred to an oven for drying at 100 °C for 20 min. The dried strips were then weighed, and its water solubility (WS) can be calculated using the following equation:

$$WS = 100 \times \frac{S - S0}{S0} \quad (1)$$

where S is initial dry mass (g) while $S0$ is final dry mass (g).

Mechanical properties

The mechanical properties of the produced films were determined by means of their tensile characteristics. Tensile index, which is normalized by sheet grammage, was chosen to report the mechanical properties rather than tensile strength, which is normalized by sheet cross-sectional area. This avoids the problem of defining the thickness of nanocellulose films, which have rough, compressible surfaces. The strips (100 mm × 15 mm) were cut from the films and tested using an Instron universal testing machine (Model 5566, USA). The test was conducted according to ASTM D 882–02 at 23 °C and 50% relative humidity (RH) (ASTM D, 882-02 2002), the tensile index of the films was calculated as following:

$$\text{Tensile Index (kN m/g)} = \frac{\text{T}\prime}{\text{R}} \quad (2)$$

where T′ is the tensile strength (kN/m) and R is the basis weight (g/m^2).

Additionally, all the films were immersed in water and their average wet tensile index was calculated by using the above-mentioned procedure.

Moisture barrier characteristics

Moisture barrier characteristics of the films were determined as water vapor permeability (WVP) in accordance with ASTM E96/E96M-05 (E. ASTM, 96/96M-05 2005). Initially, the films were cut into circles (76 mm diameter) and dried at 105 °C for 4 h to ensure complete removal of any moisture. For each sample 5 non-corroding cups were used, with 3 of them were filled with approximately 40 g of anhydrous calcium chloride ($CaCl_2$) while the remaining two cups used as blank. The circular films from each sample were then sealed on the open side of the cups, forming an airtight assembly and each of them weighed before transferring to a humidity control chamber. The test was performed at 23 °C and 50% RH and the weight of assemblies were recorded at regular time intervals. The slop of line between the weight and time was used to calculate water vapor transmission rate (WVTR). Finally, the water vapor permeability (WVP) can be determined by normalizing the WVTR with the thickness of the films. The WVP of all the films can be calculated as:

$$\text{WVTR} = \frac{\text{G}}{\text{t} \times \text{A}} \quad (3)$$

where $\frac{\text{G}}{\text{t}}$ refers to the slope of a straight line (g h^{-1}) and A is the surface area of the films (m^2). The permeance of the films can be calculated as:

$$\text{Permeance} = \frac{\text{WVTR}}{\text{S(R1} - \text{R2)}} \quad (4)$$

where S is the saturation vapor pressure per mmHg (1.333×10^2 Pa) at the tested temperature, R1 is the relative humidity of the source and R2 is the relative humidity of the vapor sink, expressed as a fraction. Finally, the WVP of the films can be calculated as:

$$\text{WVP} = \text{Permeance} \times \text{Thickness} \quad (5)$$

Characterizations

All the films were iridium coated and their microscopic morphology was determined using scanning electron microscopy (Magellan FEGSEM 400, FEI, USA) at an accelerating voltage of 5 kV and the magnifications ranging from 10,000× to 80,000×. The macroscopic morphology was evaluated using an optical profilometer (OLS5000, Olympus, Japan) at both sides of films with a 5× and 10× objective respectively.

The bulk density (ρ_{bulk}) of film samples was calculated by determining their weight, length, width, and thickness. We conducted helium pycnometer test (Micromeritics AccuPyc 1330) to measure samples' skeletal density (where $\rho_{skeletal}$ is

skeletal density). The porosity ε (%) was calculated as follows:

$$\varepsilon(\%) = 1 - \frac{\rho_{bulk}}{\rho_{skeletal}} \quad (6)$$

where ρ_{bulk} is the bulk density and ρskeletal is skeletal density.

Additionally, measurement of nitrogen adsoption-desorption isotherms was calculated by Brunauer–Emmett–Teller (BET) method through nitrogen porosimetry using Micromeritics TriStar II. Samples were degassed for 24 h at 105 °C before inserting in Micromeritics TriStar II.

Surface hydrophobicity

A Dataphysics Contact Angle Measurement System (Germany) was used to determine the static contact angles of deionized water on both sides of the films. All the contact angle tests were conducted at 23 °C and 50% RH. A 5 µl deionized water droplet was dropped on the surface of the films and the contact angle was measured for each 10 s for a total of 120 s. Moreover, the contact angle of the films didn't change much during the measurement period.

Results and discussion

Optimization of AKD content

The NC/CMC films produced via spray deposition were completely disintegrated when saturated with water; this is because the hydrophilic groups from CMC can establish hydrogen linkage with water (Shahbazi et al. 2016). To overcome this issue, the hydrophobicity of NC/CMC composite films needs to be improved. For this purpose, AKD was deposited on the fully dried NC/CMC films via spray deposition at different concentrations. The AKD depositing via spray deposition is preferred over bulk addition for producing a controlled thin layer on the films' surface and for the continuity and practicality of the process. The AKD deposited NC/CMC films were subjected to water solubility test and the results are displayed in Fig. 1. As the figure illustrates, the percentage mass loss was in the range of 12–22% for the films immersed in water for 24 h. It was observed that

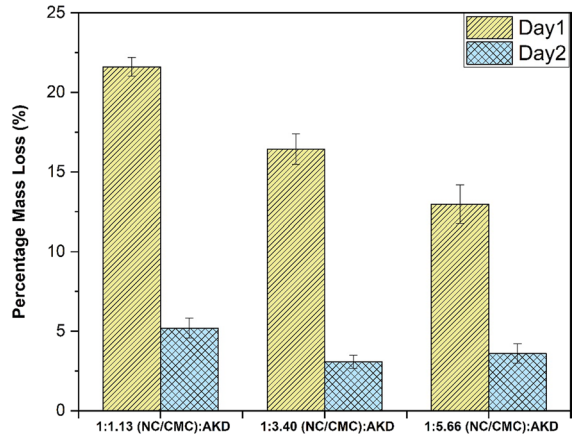

Fig. 1 Optimizing the AKD content based on percentage mass loss of the fully dried films after day1 and day 2

increasing the AKD content reduced the weight loss of the resultant films. The weight loss attributes to the CMC solubilization in water owing to its polar nature. Nevertheless, the films were quite stable and showed considerably less mass loss after day 2 (3–5%) compared with the mass loss observed after 24 h (Fig. 1). No statistically significant change was observed in the percentage mass loss of the films for the 1: 3.40 (NC/CMC): AKD and 1: 5.66 (NC/CMC): AKD samples after day 2, indicating that 1: 3.40 (NC/CMC): AKD is the optimized concentration of AKD for this study (Fig. 1).

Basis weight and thickness

At optimized concentration of AKD, two approaches were used to produce hydrophobic films: a) AKD deposition on fully dried NC/CMC films (AKD treated fully dried NC/CMC films and b) AKD deposition on partially dried NC/CMC films (AKD treated partially dried NC/CMC films). Initially, the basis weight and thickness of the films produced via these two approaches were calculated, and the results are illustrated in Fig. 2. The basis weight of the NC/CMC films was approximately 39.5 ± 1.0 g/m^2 while their thickness varied between 62 ± 2.5 µm. These values are quite similar to the ones reported in the literature (Nadeem et al. 2020). Additionally, the introduction of AKD increased the basis weight and thickness of the films to a considerable extent due to its debonding with NC and CMC while increasing the coat layer

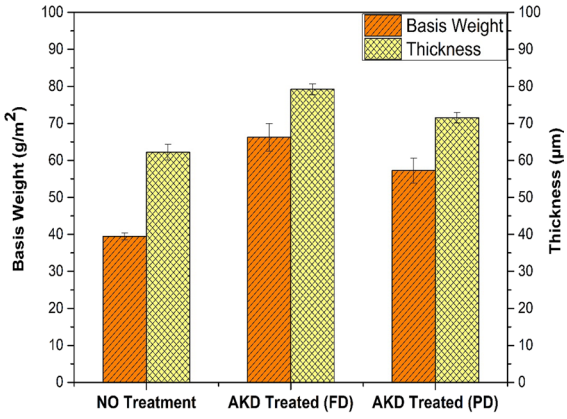

Fig. 2 Effect of AKD treatment on the basis weight and thickness of the NC/CMC films

(Fig. 2). The basis weight of AKD treated FD films was higher as compared with the AKD treated PD films owing to the reason that the fully dried films had better capacity to absorb a layer of AKD than a partially wetted film. This resulted in a separate thick layer at the top of the dried films. Additionally, the fully dried samples have better drying capacity as the AKD can penetrate all the way through the structure. Moreover, the basis weight shows a directly proportional relationship to the thickness of the films (Shanmugam et al. 2018).

Characterizations

The morphological changes of the neat and modified NC/CMC films (treated side) are displayed in Fig. 3, while the SEM images of these films at different regions and magnifications are included in the supplementary information (Figure S2). The unmodified NC/CMC film forms a kind of embedded matrix (Fig. 3A); indicating these films should have excellent moisture barrier properties as reported in the literature (Mandal and Chakrabarty 2018; Nadeem et al. 2020). However, when the films were treated with AKD, crystal-like structures combining NC, CMC and AKD could be observed. These structures are found mostly on the surface for AKD treated FD films (Fig. 3B), while these crystal-like structures can also be seen in the matrix of the films for AKD treated PD samples (Fig. 3C). Moreover, these crystal-like structures were more numerous in AKD treated PD films as compared with AKD treated FD samples. This might be due to the overflowing of the AKD suspension from the surface of fully dried films. Additionally, the non-uniformity of the NC/CMC dried film is another reason for the limited deposition of crystal-like structures on AKD treated FD films.

According to the helium pycnometry results, spraying AKD on NC/CMC films showed lower porosity for the AKD treated PD films as compared with the AKD treated FD films. This result agrees with the evidence that AKD suspension is more uniformly distributed in AKD treated PD films and may possibly have lower WVP due to their lower porosity (Table 1).

According to the results of nitrogen adsorption–desorption isotherms, the BET specific surface area (SBET) and pore volume (Vp) of the AKD treated FD films were higher than those of the AKD treated PD films. In addition, the pore size (dp) of the AKD treated FD films was 18.6 nm (Table 2), which is larger than that of AKD treated PD films (16.6 nm). These results suggest that AKD filled more pores and are uniformly distributed for AKD treated PD films. This led to the lower SBET and pore volume, and smaller pore sizes of the AKD treated PD films compared to the AKD treated FD films (Table 2). These results are also in accordance with the helium pycnometry result and SEM as discussed above.

Figure 4 shows the optical profilometry images of neat and AKD modified NC/CMC films; it indicates the decrease in aerial roughness (S_a) of AKD treated films. The change in S_a for AKD treated FD and PD films was quite significant for the rough side at higher magnification (10×); i.e., the Sa values were approximately half as compared with the neat NC/CMC films. Considering the smooth surface, the AKD treated PD films showed the least S_a values (4.04 nm), while AKD treated FD films indicated slight improvement in their roughness values (5.78 nm) as compared with neat NC/CMC films (8.16 nm). Additionally, based on physical observation, no shrinkage was observed for AKD treated PD films, while AKD treated FD films showed slight shrinkage. The long alkyl chains on the AKD surface improved the heat resistivity of the resultant composite (Nadeem et al. 2020 (b); Ryu et al. 2020). The transmittance of the AKD treated films was also observed to be lower as compared with the neat NC/CMC films. This might be due to the reduced transmission coefficient of these

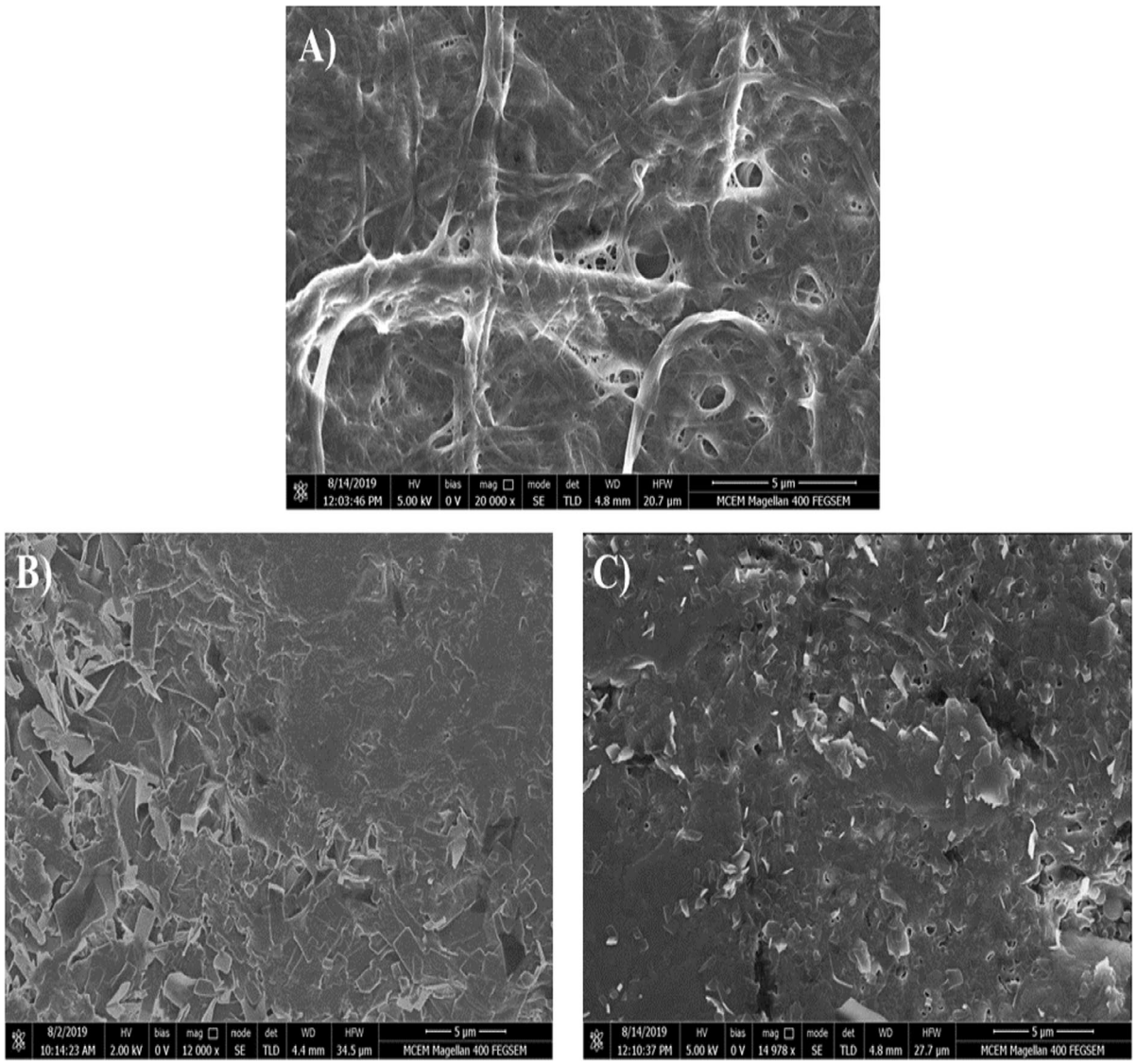

Fig. 3 SEM images of **A** neat NC/CMC film, **B** AKD treated (FD) film and **C** AKD treated (PD) film

Table 1 Porosity, bulk, and skeletal densities of samples

Entry	Sample	ρ_{bulk}(g/cm^3)	$\rho_{skeletal}$(g/cm^3)	Porosity ϵ(%)
1	NC/CMC film	1.5300	0.8500	44.4000
2	AKD treated FD films	1.3152	0.7300	44.6000
3	AKD treated PD films	1.3063	0.8500	33.4000

films on addition of AKD as reported by Fedorov et al. (Fedorov et al. 2020). Additionally, increasing film's basis weight and thickness on treatment with AKD explains the loss of transmittance (González et al. 2017).

Water contact angle

The contact angle (CA) can be measured to determine the change in the surface hydrophobicity of a biodegradable film. The CA for neat NC, CMC,

Table 2 Structural properties of AKD treated films

Entry	Sample	S_{BET} (m^2/g)	[a]d_p (nm)	V_p (cm^3/g)
1	AKD treated FD films	0.2700	18.6000	0.0021
2	AKD treated PD films	0.2500	16.6000	0.0016

[a]Adsorption average pore diameter (4 V/A by BET)

neat and modified NC/CMC films were determined, and the results are presented in Fig. 5. The fibrous NC and CMC usually have low CA values (Fig. 5), due to hydrophilic composition of these materials (Aulin et al. 2010; Shahbazi et al. 2016). However, when these materials i.e., NC and CMC were combined to produce a composite NC/CMC film, the contact angle values started to increase. As seen in Fig. 5, the CA measured on both sides of neat NC/CMC film did not change considerably and was in the range of $80° \pm 3$. The deposition of AKD on NC/CMC films has enhanced the CA values up to approximately 60% and the films were found to be highly hydrophobic. This increased hydrophobicity of AKD treated films attributes to the long alky chains of AKD on the surface of NC due to ketoester linkage as suggested by earlier studies (Song et al.

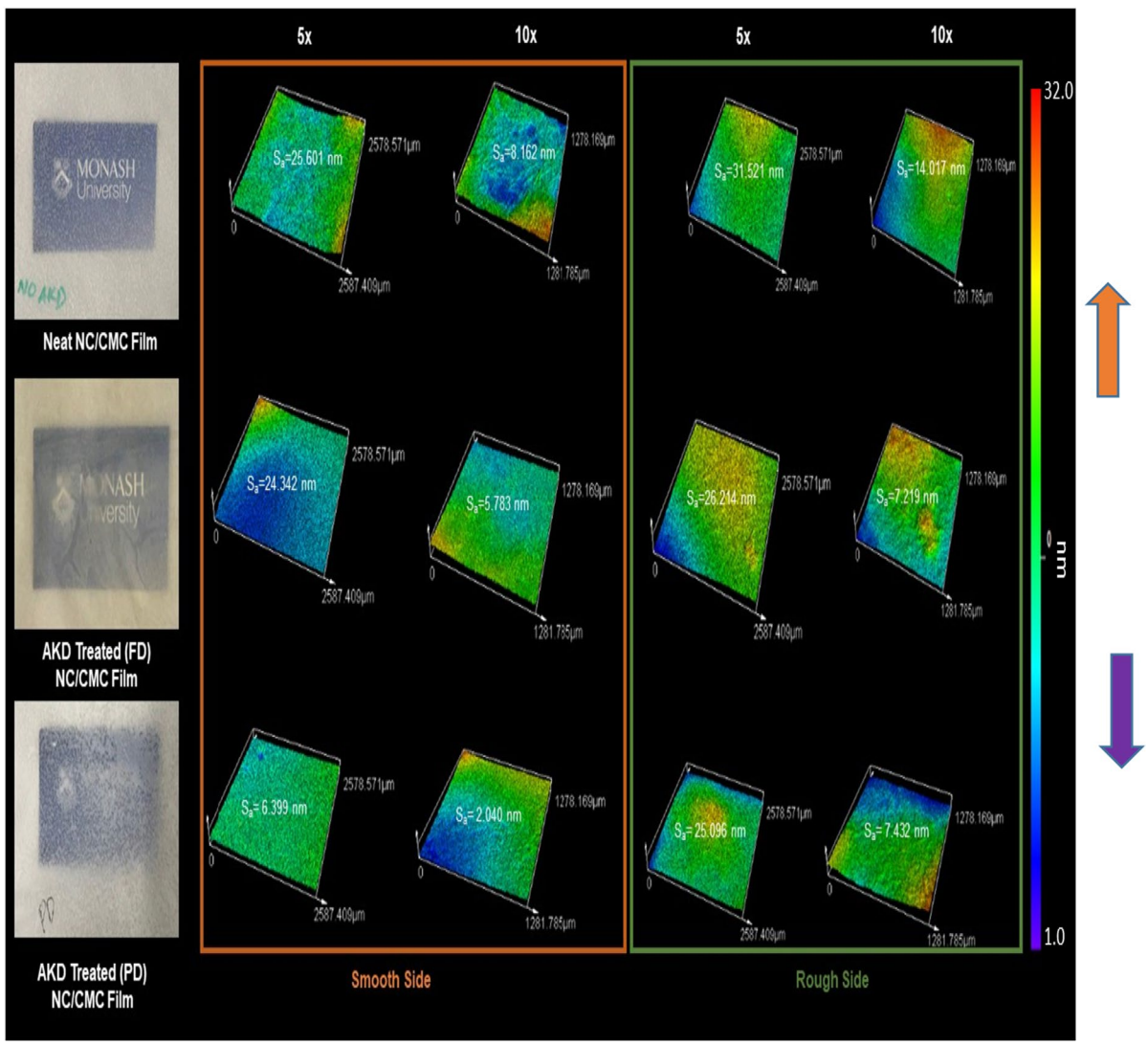

Fig. 4 Optical Profilometry images of neat and modified AKD treated films at 5× and 10×. Up arrow: Increased Roughness, Down arrow: Decreased Roughness

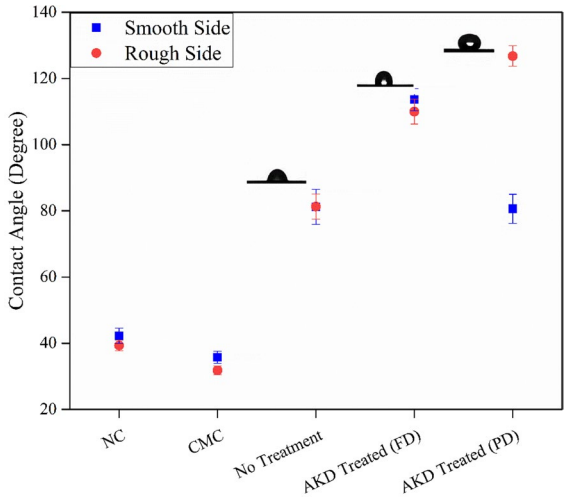

Fig. 5 Contact angle values of neat and AKD treated NC/CMC films

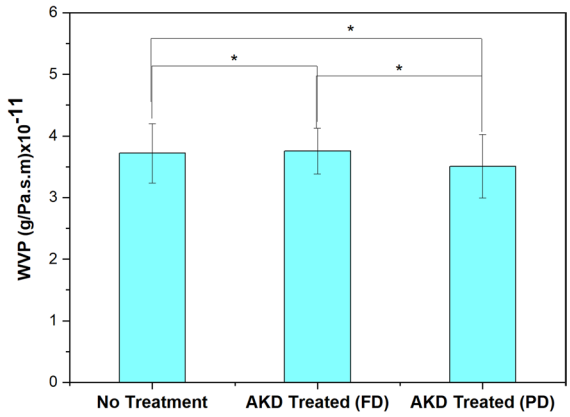

Fig. 6 WVP of neat and AKD treated NC/CMC films. Values represent the mean ± SD, n = 5, $*P > 0.05$ (obtained by Student's *t*-test)

2012; Yang et al. 2014). Additionally, the CA values (θ = 127° ± 3) for rough side (exposed to spraying) in AKD treated PD films were greater than AKD treated FD films (θ = 110° ± 5) for. The higher CA values for AKD treated PD films are due to considerably more and uniform AKD deposition as also seen from SEM images. The CA value of 128° attained almost a superhydrophobic character, which initiates at a water-contact angle of 150° (Sousa and Mano 2013). Additionally, the CA values for both smooth and rough sides didn't change significantly for AKD treated FD films. This is due to the reason that as the films were fully dried and they were not completely sticking to the substrate. This causes the AKD suspension to penetrate through the edges of the assembly, resulting in increased CA on both sides of films. Contrary, AKD treated PD films showed a significant increase in contact angle values on one side only (rough side). This variation in CA values also explains the higher basis weight of AKD treated FD films, indicating that the AKD suspension penetrates well on the surface of fully dried films. Interestingly, the CA values (θ = 78° ± 4) calculated for smooth side AKD treated PD films was in the same range as neat NC/CMC films. This indicates that AKD suspension might not have penetrated through the partially dried NC/CMC films, and thus imparting hydrophobicity on one side only.

Moisture barrier performance

The water barrier performance of a film in protective coating or in packaging can increase shelf life of the products (Shahbazi et al. 2016). The moisture barrier performance of the films was evaluated by means of water vapor permeability (WVP) and the results are illustrated in Fig. 6. The average WVP of the NC/CMC films was of 3.8×10^{-11} g/Pa.s.m. These values are quite similar to the ones reported in the literature (Mandal and Chakrabarty 2018; Nadeem et al. 2020). The moisture barrier performance was almost similar for AKD treated fully dried NC/CMC films. Additionally, no statistically significant difference in terms of WVP was observed between untreated and AKD treated NC/CMC films.

Water solubility

The water solubility test is an important criterion for the disintegration of the films and is measured as percentage mass loss. As NC and CMC are both hydrophilic polymers, any enhancement in their resistance to moisture and improved water resistance is critical. The results of water solubility test for AKD treated NC/CMC films are represented in Fig. 7. The percentage mass loss after 24 h immersion in water for the AKD deposited fully dried films was approximately 14% as compared with the AKD deposited partially dried films (≃ 11%). For day 2, a similar trend was observed regarding the percentage mass loss values

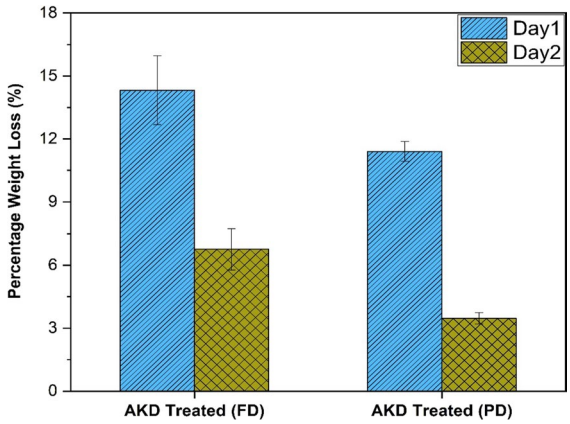

Fig. 7 Percentage mass loss for AKD treated fully dried and partially dried films

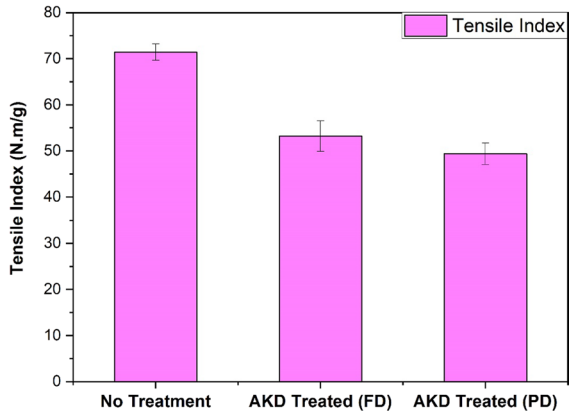

Fig. 8 Tensile index values for neat and AKD treated NC/CMC films

i.e., approximately 7% and 3% for AKD treated FD and PD films respectively. The percentage mass loss for AKD deposited FD films was quite similar to the values obtained in the optimization stage (Fig. 1). The mass loss in AKD treated films might be due to the loss of CMC filler, leaching out from the surface of the films when saturated with water. This mass loss might also cause a reduction in mechanical properties of these AKD treated films in wet conditions. The low percentage of mass loss for AKD deposited on partially dried films was due to uniform distribution of AKD, as confirmed by the SEM.

Mechanical properties

The mechanical properties of the films are mainly affected by the inter and intramolecular interactions between polymer chains (Shahbazi et al. 2016). The average tensile index values of neat and AKD treated NC/CMC films are displayed in Fig. 8. The neat NC/CMC films showed an average tensile index of 72 Nm/g for a basis weight of 40 g/m^2, which is similar to the values reported in the literature (Mandal and Chakrabarty 2018). However, the average tensile index values for AKD treated films decreased by 26–29%. Decreasing in tensile index is due to the addition of AKD affecting the bonding between the fibres. Additionally, AKD treatment has enhanced the rigidity and thus reducing the tensile index of the films (González et al. 2017). Drying at higher temperature (100° C) might also contribute to the drop in the tensile index via deteriorations of the NC fibres (Nadeem et al. 2020). The AKD treated PD films have slightly lower average tensile index values than the AKD treated FD, but the results were not statistically significant.

The average tensile index (wet), young's modulus and strain at break (%) for neat and AKD treated NC/CMC films are shown in Table 3. The AKD treated films showed significantly lower young's modulus values as compared with the neat NC/CMC films, indicating an enhanced flexibility of these films and resulting in a plasticizing effect. The young's modulus in wet state for AKD treated films was also lower (36–50%) as compared with the neat NC/CMC films. Considering the wet strength, NC/CMC films completely disintegrated in water; however, AKD treated films have shown some resistance when immersed in water (4.5–5.7 Nm/g) (Table 3). The average tensile index for wet AKD treated films has reduced significantly that might be due to the loss of CMC filler in contact with water. Additionally, when the films were immersed in water, it can penetrate through the surface from all directions and thus reducing the strength.

Conclusion

This research was conducted to improve the hydrophobicity of NC/CMC films while maintaining their dimensional stability and barrier properties. For this purpose, the effect of AKD deposition on NC/CMC films via spray deposition technique was investigated.

Table3 Mechanical Properties of neat and modified NC/CMC Films

State	Property	Neat NC/CMC	AKD Treated (FD)	AKD Treated (PD)
Dry	Young's Modulus (MPa)	6966.9 ± 145.4	1602.5 ± 350.1	1553.70 ± 386.4
Wet	Tensile Index, (Nm./g)	–	5.8 ± 1.2	4.5 ± 2.3
	Young's Modulus (MPa)	110.8 ± 21.3	70.8 ± 20.0	56.2 ± 10.8

The deposition of AKD has improved the hydrophobicity of the films to a significant extent, i.e., the AKD treated films have shown up to 60% increase in contact angle values as compared with the original NC/CMC films. The AKD deposited NC/CMC have also maintained their dimensional stability and moisture barrier properties. Overall, AKD treated partially dried NC/CMC films showed better results as compared with the AKD treated fully dried films. These treated partially dried films showed better water resistance as the percentage mass loss was approximately 4% after 2 days of immersion in water. Additionally, these AKD treated partially dried films impart hydrophobicity to one side only, i.e., the resultant films are one side hydrophilic and other side hydrophobic. These characteristics of AKD treated films present an attractive and sustainable alternative to the petroleum-based packaging for food, pharmaceutical and moisture barrier applications.

Author Contributions All authors contributed to the study conception and design. Material preparation, data collection and analysis were performed by Humayun Nadeem, Mostafa Dehghani, and Mahdieh Pazirofteh. The first draft of the manuscript was written by Humayun Nadeem and all authors commented on previous versions of the manuscript. All authors read and approved the final manuscript.

Funding Open Access funding enabled and organized by CAUL and its Member Institutions. The authors would like to express their gratitude to the Australian Research Council and the ARC Research Hub for Processing Lignocellulosics into High Value Products (PALS) for their financial support through the Industry Transformation Research Hub Grant No. E06102. The authors are also grateful to the Monash Centre for Electron Microscopy (MCEM) for availing their facilities.

Declarations

Conflict of Interest The authors have no competing interests to declare that are relevant to the content of this article.

References

AS/NZS-426 (1994) Determination of thickness and apparent bulk density or apparent sheet density

ASTM D, 882-02 (2002) Standard Test Method for tensile properties of thin plastic sheeting. In. West Conshohocken, PA

ASTM, E., 96/96M-05 (2005) Standard test methods for water vapor transmission of materials. In. West Conshohocken, PA

Aulin C, Gällstedt M, Lindström T (2010) Oxygen and oil barrier properties of microfibrillated cellulose films and coatings. Cellulose 17:559–574. https://doi.org/10.1007/s10570-009-9393-y

Bai B, Jin H, Fan C, Cao C, Wei W, Cao W (2019) Experimental investigation on liquefaction of plastic waste to oil in supercritical water. J Waste Manag 89:247–253. https://doi.org/10.1016/j.wasman.2019.04.017

DeLoid GM, Cao X et al (2019) Toxicological effects of ingested nanocellulose in in vitro intestinal epithelium and in vivo rat models. Environ Sci Nano 6:2105–2115. https://doi.org/10.1039/C9EN00184K

Fedorov PP, Luginina AA, Kuznetsov SV et al (2020) Hydrophobic up-conversion carboxylated nanocellulose/fluoride phosphor composite films modified with alkyl ketene dimer. Carbohydr Polym 250:116866. https://doi.org/10.1016/j.carbpol.2020.116866

Foster EJ, Moon RJ et al (2018) Current characterization methods for cellulose nanomaterials. Chem Soc Rev 47:2609–2679. https://doi.org/10.1039/C6CS00895J

Geyer R, Jambeck JR, Law KL (2017) Production, use, and fate of all plastics ever made. Sci Adv 3:e1700782. https://doi.org/10.1126/sciadv.1700782

González I, Oliver-Ortega H, Tarrés Q, Delgado-Aguilar M, Mutjé P, Andreu D (2017) Immobilization of antimicrobial peptides onto cellulose nanopaper. Int J Biol Macromol 105:741–748. https://doi.org/10.1016/j.ijbiomac.2017.07.094

Gregorová A, Saha N, Kitano T, Sáha P (2015) Hydrothermal effect and mechanical stress properties of carboxymethylcellulose based hydrogel food packaging. Carbohydr Polym 117:559–568. https://doi.org/10.1016/j.carbpol.2014.10.009

Hammond GP, Jones CI (2008) Embodied energy and carbon in construction materials. P I CIVIL ENG-ENERGY 161:87–98. https://doi.org/10.1680/ener.2008.161.2.87

Hideno A, Abe K, Uchimura H, Yano H (2016) Preparation by combined enzymatic and mechanical treatment and characterization of nanofibrillated cotton fibers. Cellulose 23:3639–3651. https://doi.org/10.1007/s10570-016-1075-y

Ho BT, Roberts TK, Lucas S (2018) An overview on biodegradation of polystyrene and modified polystyrene: the microbial approach. Crit Rev Biotechnol 38:308–320. https://doi.org/10.1080/07388551.2017.1355293

Jang J-H, Lee S-H, Endo T, Kim NH (2015) Dimension change in microfibrillated cellulose from different cellulose sources by wet disk milling and its effect on the properties of PVA nanocomposite. Wood Sci Technol 49:495–506. https://doi.org/10.1007/s00226-015-0703-2

Khan A, Huq T, Khan RA, Riedl B, Lacroix M (2014) Nanocellulose-based composites and bioactive agents for food packaging. Crit Rev Food Sci Nutr 54:163–174. https://doi.org/10.1080/10408398.2011.578765

Kumar S, Chauhan VS, Chakrabarti SK (2016) Separation and analysis techniques for bound and unbound alkyl ketene dimer (AKD) in paper: A review. Arab J Chem 9:S1636–S1642. https://doi.org/10.1016/j.arabjc.2012.04.019

Lavoine N, Desloges I, Khelifi B, Bras J (2014) Impact of different coating processes of microfibrillated cellulose on the mechanical and barrier properties of paper. J Mater Sci 49:2879–2893. https://doi.org/10.1007/s10853-013-7995-0

Lebreton L, Andrady A (2019) Future scenarios of global plastic waste generation and disposal. Palgrave Commun 5:6. https://doi.org/10.1057/s41599-018-0212-7

Lee SY, Chun SJ, Kang IA, Park JY (2009) Preparation of cellulose nanofibrils by high-pressure homogenizer and cellulose-based composite films. J Ind Eng Chem 15:50–55. https://doi.org/10.1016/j.jiec.2008.07.008

Li F, Mascheroni E, Piergiovanni L (2015) The potential of nanocellulose in the packaging field: A review. Packag Technol Sci 28:475–508. https://doi.org/10.1002/pts.2121

Liu S, Low ZX et al (2019) Enhancement of desalination performance of thin-film nanocomposite membrane by cellulose nanofibers. J Membr Sci 592:117363. https://doi.org/10.1016/j.memsci.2019.117363

Mandal A, Chakrabarty D (2018) Studies on mechanical, thermal, and barrier properties of carboxymethyl cellulose film highly filled with nanocellulose. J Thermoplast Compos Mater 32:995–1014. https://doi.org/10.1177/0892705718772868

Miri S, Nadeem H, Hora Y, Chin BWX, Andrews PC, Batchelor W (2022) Depth filtration application of nanofibrillated cellulose-mesoporous silica nanoparticle composites as double-layer membranes. J Environ Chem Eng 10:106892. https://doi.org/10.1016/j.jece.2021.106892

Miri S, Raghuwanshi VS, Andrews PC, Batchelor W (2021) Composites of mesoporous silica precipitated on nanofibrillated cellulose and microfibrillated cellulose: Effect of fibre diameter and reaction conditions on particle size and mesopore diameter. Micropor Mesopor Mat 311:110701. https://doi.org/10.1016/j.micromeso.2020.110701

Muñoz RA, Cabrera-Papamija G, Machuca-Martínez F, Rodríguez LA, Diosa JE, Mosquera-Vargas E (2022) Plastic recycling and their use as raw material for the synthesis of carbonaceous materials. Heliyon 8:e09028. https://doi.org/10.1016/j.heliyon.2022.e09028

Nadeem H, Athar M, Dehghani M, Garnier G, Batchelor W (2022a) Recent advancements, trends, fundamental challenges and opportunities in spray deposited cellulose nanofibril films for packaging applications. Sci Total Environ 836:155654. https://doi.org/10.1016/j.scitotenv.2022.155654

Nadeem H, Dehghani M, Garnier G, Batchelor W (2022b) Life cycle assessment of cellulose nanofibril films via spray deposition and vacuum filtration pathways for small scale production. J Clean Prod 342:130890. https://doi.org/10.1016/j.jclepro.2022.130890

Nadeem H, Habib NZ, Ng CA, Zoorob SE, Mustaffa Z, Chee S, Younas M (2017) Utilization of catalyzed waste vegetable oil as a binder for the production of environmentally friendly roofing tiles. J Clean Prod 145:250–261. https://doi.org/10.1016/j.jclepro.2017.01.028

Nadeem H, Naseri M, Shanmugam K, Browne C, Garnier G, Batchelor W (2020) Impact of heat drying on the physical and environmental characteristics of the nanocellulose-based films produced via spray deposition technique. Cellulose 27:10225–10239. https://doi.org/10.1007/s10570-020-03473-3

Nadeem H, Naseri M et al (2020) An energy efficient production of high moisture barrier nanocellulose/carboxymethyl cellulose films via spray-deposition technique. Carbohydr Polym 250:116911. https://doi.org/10.1016/j.carbpol.2020.116911

Nechyporchuk O, Belgacem MN, Bras J (2016) Production of cellulose nanofibrils: a review of recent advances. Ind Crops Prod 93:2–25. https://doi.org/10.1016/j.indcrop.2016.02.016

Nogi M, Iwamoto S, Nakagaito AN, Yano H (2009) Optically transparent nanofiber paper. Adv Mater 21:1595–1598. https://doi.org/10.1002/adma.200803174

Raj P, Blanco A, de la Fuente E, Batchelor W, Negro C, Garnier G (2017) Microfibrilated cellulose as a model for soft colloid flocculation with polyelectrolytes. Colloid Surf A-Physicochem Eng ASP 516:325–335. https://doi.org/10.1016/j.colsurfa.2016.12.055

Ryu YS, Lee JH, Kim SH (2020) Efficacy of alkyl ketene dimer modified microcrystalline cellulose in polypropylene matrix. Polym 196:122463. https://doi.org/10.1016/j.polymer.2020.122463

Savadekar N, Karande V, Vigneshwaran N, Bharimalla A, Mhaske S (2012) Preparation of nano cellulose fibers and its application in kappa-carrageenan based film. Int J Biol Macromol 51:1008–1013. https://doi.org/10.1016/j.ijbiomac.2012.08.014

Shahbazi M, Ahmadi SJ, Seif A, Rajabzadeh G (2016) Carboxymethyl cellulose film modification through surface photo-crosslinking and chemical crosslinking for food

packaging applications. Food Hydrocoll 61:378–389. https://doi.org/10.1016/j.foodhyd.2016.04.021

Shak KPY, Pang YL, Mah SK (2018) Nanocellulose: recent advances and its prospects in environmental remediation. Beilstein J Nanotechnol 9:2479–2498. https://doi.org/10.3762/bjnano.9.232

Shanmugam K, Doosthosseini H, Varanasi S, Garnier G, Batchelor W (2018) Flexible spray coating process for smooth nanocellulose film production. Cellulose 25:1725–1741. https://doi.org/10.1007/s10570-018-1677-7

Shanmugam K, Varanasi S, Garnier G, Batchelor W (2017) Rapid preparation of smooth nanocellulose films using spray coating. Cellulose 24:2669–2676. https://doi.org/10.1007/s10570-017-1328-4

Shimizu M, Saito T, Fukuzumi H, Isogai A (2014) Hydrophobic, ductile, and transparent nanocellulose films with quaternary alkylammonium carboxylates on nanofibril surfaces. Biomacromol 15:4320–4325. https://doi.org/10.1021/bm501329v

Siró I, Plackett D (2010) Microfibrillated cellulose and new nanocomposite materials: a review. Cellulose 17:459–494. https://doi.org/10.1007/s10570-010-9405-y

Song X, Chen F, Liu F (2012) Preparation and characterization of alkyl ketene dimer (AKD) modified cellulose composite membrane. Carbohydr Polym 88:417–421. https://doi.org/10.1016/j.carbpol.2011.10.062

Sousa MP, Mano JF (2013) Patterned superhydrophobic paper for microfluidic devices obtained by writing and printing. Cellulose 20:2185–2190. https://doi.org/10.1007/s10570-013-9991-6

Stephen AM (1995) Food polysaccharides and their applications (vol 67). CRC Press, Boca Raton

Takihara T, Yoshida Y, Isogai A (2007) Reactions between cellulose diacetate and alkenylsuccinic anhydrides and characterization of the reaction products. Cellulose 14:357–366. https://doi.org/10.1007/s10570-007-9112-5

Varanasi S, He R, Batchelor W (2013) Estimation of cellulose nanofibre aspect ratio from measurements of fibre suspension gel point. Cellulose 20:1885–1896. https://doi.org/10.1007/s10570-013-9972-9

Yan Y, Amer H et al (2016) Dry, hydrophobic microfibrillated cellulose powder obtained in a simple procedure using alkyl ketene dimer. Cellulose 23:1189–1197. https://doi.org/10.1007/s10570-016-0887-0

Yang Q, Takeuchi M, Saito T, Isogai A (2014) Formation of nanosized islands of dialkyl β-ketoester bonds for efficient hydrophobization of a cellulose film surface. Langmuir 30:8109–8118. https://doi.org/10.1021/la501706t

Yoshida Y, Isogai A (2013) Nanofibrillation of alkyl ketene dimer (AKD)-treated cellulose in tetrahydrofuran. Cellulose 20:3–7. https://doi.org/10.1007/s10570-012-9826-x

Zhang F, Zhao Y et al (2021) Current technologies for plastic waste treatment: a review. J Clean Prod 282:124523. https://doi.org/10.1016/j.jclepro.2020.124523

Zhang H, Yang Y, Dai W, Lu S, Yu H, Ji Y (2014) Size-controlled Pd nanoparticles supported on α-Al2O3 as heterogeneous catalyst for selective hydrogenation of acetylene. Chin J Chem Eng 22:516–521. https://doi.org/10.1016/S1004-9541(14)60070-7